Future material demand for global silicon-based PV modules under net-zero emissions target until 2050

Xu, Chengjian; Isabella, Olindo; Vogt, Malte Ruben

DOI
10.1016/j.resconrec.2024.107824

Publication date
2024

Document Version
Final published version

Published in
Resources, Conservation and Recycling

Resources, Conservation & Recycling 210 (2024) 107824

Contents lists available at ScienceDirect

Resources, Conservation & Recycling

journal homepage: www.sciencedirect.com/journal/resources-conservation-and-recycling

Full length article

Future material demand for global silicon-based PV modules under net-zero emissions target until 2050

Chengjian Xu [a,b,*], Olindo Isabella [a], Malte Ruben Vogt [a]

[a] Photovoltaic Materials and Devices, Delft University of Technology, 2628CD, Delft, The Netherlands
[b] Institute of Environmental Sciences (CML), Leiden University, 2300RA, Leiden, The Netherlands

ARTICLE INFO

Keywords:
dMFA
Material demand
Critical raw materials
Silicon-based photovoltaic modules
Photovoltaic module efficiency
Closed-loop recycling

ABSTRACT

The surge in global solar photovoltaic (PV) deployment as a measure to combat climate change is undeniable. However, this growth comes with its own set of challenges, particularly concerning the materials required for silicon-based PV modules. In this study, we quantify future material demand for silicon-based PV modules, considering technological advancements in PV module efficiency and material intensity. The annual material demand is projected to increase significantly for indium (38–286 times), silver (4–27 times), and other materials (2–20 times) over the period from 2022 to 2050, depending on PV deployment scenarios. Indium and silver demand are notably influenced by PV technology choice. Cumulative indium demand during 2022–2050 could range from 0 kt (for 100 % passivated emitter and rear contact or tunnel oxide passivated contact PV) to 209 kt (for 100 % perovskite-silicon four-terminal tandem PV). Cumulative silver demand during the same period could vary from 144 kt (for 100 % passivated emitter and rear contact PV) to 1121 kt (for 100 % silicon heterojunction PV). One promising approach to mitigate the increasing demand for primary materials is closed-loop recycling. By implementing efficient PV collection and recycling processes, cumulative primary material demand could be reduced by 10 % to 30 % between 2022 and 2050.

1. Introduction

Driven by global commitments to climate change goals and low-cost energy sources (Yuan et al., 2022), global photovoltaic (PV) deployment has surged from only 1.2 GW_p in 2000 to 1046 GW_p in 2022 (IRENA, 2023b). During the same period, there has been a 95 % reduction in PV module cost, plummeting from 5 USD per Watt to 0.25 USD per Watt (BloombergNEF, 2022). This impressive trajectory is largely attributed to the continuous technological advancements across various PV technologies. However, most of the advancements have focused on silicon-based PV, which currently dominates the market with a share of approximately 95 % (Ballif et al., 2022; European et al., 2022). Silicon-based PV is projected to maintain its dominant position due to its superior efficiency and reliability (Zhou et al., 2022).

Silicon-based PV relies on a diverse range of raw materials, including silicon, tin, aluminum, copper, indium, silver, lead, glass, plastics, and others (IEA, 2022a). Some PV materials have been identified as critical and strategic, considering their economic significance, associated supply risks, and other factors (Goe and Gaustad, 2014). In 2023, the EU designated silicon, aluminum, and copper as critical raw materials (European et al., 2023), while the US classified them as near-critical materials within the medium-term horizon (2025–2035) (USDOE, 2023). The UK's critical materials list for 2022 includes tin and indium in addition to silicon (GOV.UK, 2023). China, in its National Mineral Resources Planning (2016–2020), classified aluminum, copper, and tin as strategic and critical materials (Resources, 2016).

The supply chain for PV and associated components/materials may encounter vulnerability and disruption, particularly during periods of rapid upscaling of PV deployment. This is partly because the PV supply chain is currently concentrated in specific countries or regions, such as China (IEA, 2022a). Further concerns arise from the environmental and social impacts inherent in PV materials (Dubey et al., 2013; Hernandez et al., 2014), including occupational health hazards, such as SiH_2Cl_2 and SiH_3Cl, associated with producing solar-grade silicon (Ramírez-Márquez et al., 2020). To address these concerns, securing sustainable and responsible sourcing of raw materials for PV production is crucial (Kügerl et al., 2023).

As the world increasingly turns to solar power as a key renewable energy source, understanding the associated material demands and exploring strategies for sustainable resource management become

* Corresponding author at: Photovoltaic Materials and Devices, Delft University of Technology, 2628CD, Delft, The Netherlands.
E-mail address: C.Xu@tudelft.nl (C. Xu).

https://doi.org/10.1016/j.resconrec.2024.107824
Received 2 April 2024; Received in revised form 10 July 2024; Accepted 14 July 2024
Available online 26 July 2024

imperative. Identifying critical PV materials and implementing measures to ensure a sustainable supply chain requires a comprehensive understanding of future PV material demand. While existing research acknowledges the growing demand for PV materials, it is often concentrated on specific countries/regions like the EU (European et al., 2020; Guzik et al., 2022), US (Basore and Feldman, 2022; Smith and Margolis, 2019), and China (Duan et al., 2016; Elshkaki and Shen, 2019; Ren et al., 2021), and is limited to timeframes only until 2030 (European et al., 2016; Heidari and Anctil, 2021; IRENA, 2023a) or 2040 (Nassar et al., 2016). Furthermore, some existing studies investigate only a single material, such as silver (Hallam et al., 2023; Li and Adachi, 2019; Lo Piano et al., 2019) or indium (Choi et al., 2016; Gómez et al., 2023). These studies often utilize PV material intensity data for specific PV technologies in particular years, failing to develop dynamic material intensity for different PV technologies over time.

This study addresses research gaps by building a dynamic material flow analysis (dMFA) model for silicon-based PV modules. The novelty of the dMFA model lies in its implementation to reflect future data dynamics, rather than in the dMFA methodology itself. The model captures annual dynamics not only in PV deployment size but also in module efficiency, material compositions, and market shares for various silicon-based PV technologies until 2050. The PV technologies include aluminum back surface field (Al-BSF), passivated emitter and rear contact (PERC), tunnel oxide passivated contact (TOPCon), silicon heterojunctions (SHJ), interdigitated back contact (IBC), and perovskite-silicon tandem (please refer to Section 2.3 for detailed descriptions of each technology). This study provides a more comprehensive technology roadmap compared to existing ones, which often focus on a limited number of technologies and overlook the perovskite-silicon tandem. The dMFA model is employed to assess global demand for all PV materials until 2050 under different PV deployment scenarios, with a focus on key materials such as indium, silver, tin, silicon, aluminum, and copper. Furthermore, we compare material demand to current production capacities/known reserves and discuss potential supply chain risks related to PV materials, as well as key strategies for reducing material demand, including closed-loop recycling and material substitution. The findings underscore the imperative need for sustained improvements in PV efficiency and careful selection of PV technology to alleviate PV material demand. Overall, this paper offers essential guidance for policymakers, industry stakeholders, and researchers striving to navigate the complex interplay between PV deployment and finite resources.

2. Methods

2.1. Model overview

This study aims to develop a dMFA model to investigate material demand for global PV deployment. The investigation considers key factors of PV deployment size, lifetime, efficiency, and material compositions, etc. We use historical PV deployment capacity data from 2000 to 2022 as sourced from (IRENA, 2023b). We then compile future PV deployment scenarios with the goal of achieving net-zero emissions by 2050. The PV deployment scenarios include the share between residential and utility-scale PV installations, and different lifetimes are considered for residential and utility-scale PV. Additionally, we develop a roadmap for silicon-based PV technologies including Al-BSF, PERC, TOPCon, SHJ, IBC, and perovskite-silicon tandem (please refer to Section 2.3 for details). The roadmap provides information on PV module efficiency, market share, and dynamic material composition for each technology until 2050.

This study focuses on silicon-based PV, representing approximately 95 % of the PV market (Ballif et al., 2022; European et al., 2022; Zhou et al., 2022). Other PV technologies, such as thin-film PV, are out of the research scope. We investigate the material demand for PV modules, including both cells and the interconnection of cells into modules. Material demand for PV inverters, mounting structures, and transmission cables is not within the research scope.

2.2. PV deployment scenarios

Historical PV module deployment has increased from approximately 1 GW_p in 2000 to 100 GW_p in 2012 and further to 1000 GW_p (equal to 1 TW_p) in 2022 (IRENA, 2023b). As of 2022, global PV is estimated to generate 1.3 petawatt hours (PWh) of electricity. This constitutes 4.5 % (EMBER, 2023) of the 29 PWh (RTOInsider, 2023) worldwide electricity generation in 2022. Further progress in PV penetration is needed to achieve net-zero emissions target by 2050. We consider the future development of global electricity generation and PV's contribution to compile PV deployment scenarios until 2050.

We compile the conservative PV scenario to represent the low bound of PV deployment, which is derived from the International Energy Agency (IEA) to forecast PV deployment of 15.5 TW_p (IEA, 2021) by 2050. In this scenario, global PV generated electricity is projected to reach 24.5 PWh by 2050. This amount will constitute 35 % of the total projected global electricity generation (totally 70 PWh) in 2050. Although some greenhouse gas emissions are anticipated in 2050 under the conservative PV scenario, they are assumed to be counterbalanced by direct air capture, bioenergy utilization, or other technologies. In contrast, the optimistic PV scenario is compiled to represent the high bound of PV deployment, which is based on (Bogdanov et al., 2021) to project PV deployment of 63.4 TW_p by 2050. This scenario envisions PV's pivotal role in achieving a 100 % renewable energy system by 2050 without relying on carbon dioxide removal. In the optimistic PV scenario, PV is anticipated to provide 69 % of the global electricity generation: 103.5 PWh of PV electricity generation out of the 150 PWh global total electricity generation. We use a logistic model for estimating PV's share in global electricity generation (Lowe and Drummond, 2022) and a linear model for estimating global electricity generation between 2022 and 2050.

Additionally, we include the share between residential and utility-scale PV installations by using the IEA data until 2021 (IEA, 2022b). As of 2021, approximately 20 % of installations are residential, while 80 % are utility-scale, highlighting the dominance of utility-scale PV. This dominance is projected to persist in the future, with utility-scale installations expected to constitute about two-thirds of global capacity by 2050 (DNV, 2019). The share of residential and utility-scale PV installations from 2022 to 2050 is maintained as in the IEA data in 2021.

2.3. PV module efficiency and market share

To reduce cost and enhance PV efficiency, technological developments for silicon-based PV include the transition from p-type silicon to n-type silicon, the shift from multicrystalline silicon to monocrystalline silicon, as well as passivation improvements, structural modifications, and production equipment advancements (VDMA, 2022). We build the technology development roadmap for silicon-based PV based on International Technology Roadmap for Photovoltaic (ITRPV) data until 2030 (VDMA, 2022), and further extrapolating until 2050 by incorporating estimations from other sources (Blom et al., 2023; Hermle et al., 2020; PVmagazine, 2023). The technology development roadmap projects efficiency improvement and market share for each technology until 2050. The roadmap includes various silicon-based PV technologies, namely Al-BSF, PERC, TOPCon, SHJ, IBC, and perovskite-silicon tandem. Fig. 1 illustrates the different structures and compositions of these technologies. PERC (Sadhukhan et al., 2021) and TOPCon (Xu et al., 2022) deploy additional aluminum oxide and silicon-contained layers (silicon nitride, or silicon oxide, or poly-Si) on top of Al-BSF to enhance surface passivation and increase PV efficiency. SHJ (EPFL, 2023) utilizes amorphous silicon and indium tin oxide layers to enhance electron collection efficiency and increase PV efficiency. IBC technology features a distinct structure by placing all grid contacts on the rear side to optimize PV efficiency (VDMA, 2022). Perovskite-silicon tandem is assumed

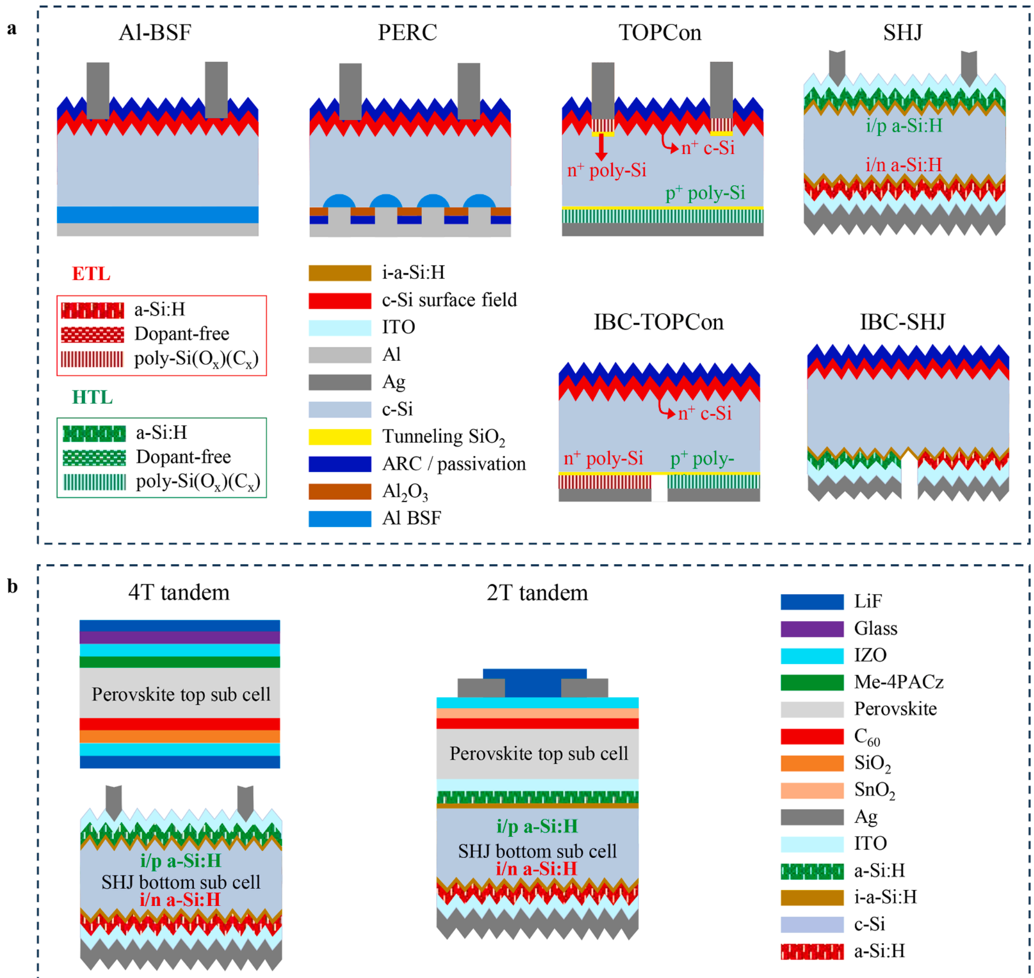

Fig. 1. Sketches of the various PV cell technologies, illustrating their different structures and compositions. Panel (**a**) includes Al-BSF, PERC, TOPCon, SHJ, and IBC (both IBC-TOPCon and IBC-SHJ). Panel (**b**) includes 4T tandem and 2T tandem technologies. Each panel has its own legend. The full names of the PV technologies are: aluminum back surface field (Al-BSF), passivated emitter and rear contact (PERC), tunnel oxide passivated contact (TOPCon), silicon heterojunctions (SHJ), and interdigitated back contact (IBC). IBC-Topcon denotes an IBC cell featuring TOPCon contacts, while IBC-SHJ indicates an IBC cell featuring SHJ contacts. Tandem technology refers to perovskite-silicon tandem technology, available in either mechanically stacked four-terminal (4T) or monolithically integrated two-terminal (2T) tandem configurations. The full names of some cell components are: electron transport layer (ETL), hole transport layer (HTL), hydrogenated amorphous silicon (a-Si:H), intrinsic hydrogenated amorphous silicon (i-a-Si:H), indium tin oxide (ITO), crystalline silicon (c-Si), anti-reflective coatings (ARC), indium zinc oxide (IZO), and [4-(3,6-dimethyl-9H-carbazol-9-yl)butyl]phosphonic acid (Me-4PACz).

to integrate a perovskite on top of a SHJ (Shrivastav et al., 2021; Tockhorn et al., 2022) to maximize PV efficiency. In this study, we assume that the tandem market is evenly split between the mechanically stacked four-terminal (4T) and monolithically integrated two-terminal (2T) tandem configurations unless stated otherwise (see Supplementary Note 1 for details). A comparative analysis between the adoption of the 2T and 4T tandem configurations is included in Fig. 5.

The assumed trend for PV module efficiency involves an annual increase of 0.5 % (Dullweber et al., 2020; Hermle et al., 2020) in an absolute number, and after a certain period, it will stabilize at a value determined by fundamental technical limitations. We establish efficiency limitations of 20 % for Al-BSF, 24 % for PERC, 26 % for both TOPCon and SHJ, 26.5 % for IBC, and 39 % for perovskite-silicon tandem modules. These mentioned efficiency limitations apply to monofacial PV modules, with bifacial PV modules set at 1.05 times the efficiency limitations of monofacial modules. The PV efficiency trend for each technology is calculated using Eq. (1), and the PV-technology-market-share-based average module efficiency is determined by Eq. (2):

$$\eta_i[t] = min\left(\eta_i[t-1] + 0.5\%,\ \eta_{i,limit}\right) \tag{1}$$

$$\eta_{avg}[t] = \sum_{i=1}^{n} \eta_i[t] * MS_i[t] \tag{2}$$

where η_i is the PV module efficiency for technology type i (in the unit of %), $\eta_{i,limit}$ is the PV module efficiency limitation for technology type i (in the unit of%), η_{avg} is the PV-technology-market-share-based average module efficiency (in the unit of%), n is the total number of PV technologies, and MS_i is the market share of technology type i (in the unit of %).

2.4. PV lifetime

The PV lifetime depends on various factors such as power degradation, technical failures, extreme weather damage, and economic considerations (Tan et al., 2022). In the case of residential PV systems, economic factors may outweigh power degradation in determining their lifespan. This is particularly notable due to the declining initial costs of new PV installations, contrasted with the rising maintenance expenses or diminishing long-term savings associated with older PV systems experiencing high power degradation. Advances in PV efficiency, coupled with incentive programs and policies, could prompt the early replacement of lower-efficiency PV systems to capture economic benefits. Residential PV systems can exhibit an average lifetime of 18 years (Tan et al., 2022). In contrast, utility-scale PV usually demonstrates a relatively longer lifetime, with an average lifetime of 26 years (Tan et al., 2022). This is because of the substantial investments associated with utility-scale PV projects, leading to delayed adoption of higher-efficiency PV technologies by industries. The modelling of utility-scale PV lifetime concentrates on the impacts of power degradation, damage, and technical failures, which is referred to as the "early loss lifetime" utilized by the IEA and International Renewable Energy Agency (Weckend et al., 2016).

We utilize the Weibull distribution to estimate the PV lifetime, as conducted in current literatures (Tan et al., 2022; Weckend et al., 2016). The Weibull lifetime distribution function is expressed as the following Eq. (3):

$$f(t) = \begin{cases} \alpha * \beta^{-\alpha} * (t-\gamma)^{\alpha-1} * e^{-\left(\frac{(t-\gamma)}{\beta}\right)^{\alpha}} & if\ t > \gamma \\ 0\ otherwise \end{cases} \quad (3)$$

where α is the shape parameter controlling the 'tail' of the distribution, β is the scale parameter known as the Weibull slope, γ is the location parameter indicating the start of obsolescence, and t is the year.

Specifically, we assign a value of 0 for γ, signifying $f(t) = 0\ if\ t \le 0$. We incorporate different shape and scale parameters for residential and utility-scale PV, as outlined in the literatures (Tan et al., 2022; Weckend et al., 2016). For residential PV, we assign values of 2.5 for α and 20 for β, while for utility PV, we utilize values of 2.5 for α and 30 for β. Note the lifetime distributions aim to highlight overall lifetime patterns for residential and utility-scale PV. The lifetime is not distinguished among different PV technologies due to a lack of specific data.

2.5. PV material compositions

This study uses the IEA's data for material compositions of Al-BSF (Frischknecht et al., 2015). The Al-BSF structure includes several key components: the front surface, which typically has an anti-reflective coating; the silicon wafer, which forms the core of the cell; and the back surface, where an aluminum layer forms the back surface field. The typical thickness of multicrystalline silicon and monocrystalline silicon wafers for Al-BSF is 180 μm and 170 μm, respectively (Frischknecht et al., 2015). Based on Al-BSF structure, we derive material compositions for other PV technologies by investigating the added layer thicknesses, content, and density, as well as the change of components such as using non-lead interconnection and adopting a glass backsheet (for bifacial PV) (VDMA, 2022). For PERC, we introduce 1 nm Al_2O_3 and 75 nm Si_3N_4 layers on top of the Al-BSF configuration (Sadhukhan et al., 2021). TOPCon incorporates 1.5 nm SiO_2 layer and 140 nm doped poly-Si layer (Xu et al., 2022). SHJ integrates a total of 130 nm indium tin oxide (ITO) layer (80 nm for the top and 50 nm for the bottom), and 30 nm amorphous silicon layer (EPFL, 2023). IBC is modeled with the same material compositions (in the unit of kg per m^2) as TOPCon or SHJ due to data limitations, despite having a different structure. This structural difference allows IBC to typically achieve slightly higher efficiency than TOPCon or SHJ due to having no shading losses as IBCs have both contacts at the rear side, which results in less material usage (in the unit of kg per Wp). Perovskite-silicon tandem utilizes SHJ as bottom cell but includes a perovskite top cell consisting of ITO (90 nm), SnO_2 (10 nm), C_{60} (23 nm), perovskite (569 nm), and Me-4PACz ([4-(3, 6-dimethyl-9H-carbazol-9-yl)butyl]phosphonic acid) (Shrivastav et al., 2021; Tockhorn et al., 2022). Please see Supplementary Note 2 for details on how we model material compositions for 2T and 4T tandem configurations.

We also examine the reduction in material mass per module area for different PV components and materials (VDMA, 2022). We consider silicon wafer thickness (WaferWorld, 2020), aluminum in rear contacts, interconnection materials, lead content, silver content (Hallam et al., 2023), front/back glass thickness, and frame materials (such as aluminum and plastics). Note that in our analysis, we assume constant thickness for added layers (Al_2O_3, Si_3N_4, ITO) due to limited available data.

We calculate the material mass per module area by the following Eq. (4) and the PV-technology-market-share-based average material mass per module area by the following Eq. (5):

$$MM_{i,j}[t] = MT_{i,j}[t] * MD_j \quad (4)$$

$$MM_j[t] = \sum_{i=1}^{n} MM_{i,j}[t] * MS_i[t] \quad (5)$$

where $MM_{i,j}$ is the material mass per module area for technology type i and material type j (in the until of kg/m^2), $MT_{i,j}$ is the material thickness for technology type i and material type j (in the unit of nm), MD_j is the material density for any technology type and material type j (in the unit of g/cm^3), MI_j is the PV-technology-market-share-based average material mass per module area for material type j (in the until of kg/m^2), and MS_i is the market share of technology type i (in the unit of%).

Material intensity is characterized as the ratio of material mass to power output under standard testing conditions for PV modules, expressed in kg per Wp. Improvement in material intensity can be achieved by increasing PV module efficiency (determining rated power in Wp per m^2) or reducing material mass per module area (measured in kg per m^2 of PV module), or a combination of both approaches. The calculation for material intensity is given by Eq. (6), and the PV-technology-market-share-based average material intensity is determined by Eq. (7):

$$MI_{i,j}[t] = \frac{MM_{i,j}[t]}{\eta_i[t] * 1000} \quad (6)$$

$$MI_j[t] = \sum_{i=1}^{n} MI_{i,j}[t] * MS_i[t] \quad (7)$$

where $MI_{i,j}$ is the material intensity for technology type i and material type j (in the until of kg/Wp), MI_j is the PV-technology-market-share-based average material intensity for material type j (in the until of kg/Wp), and MS_i is the market share of technology type i (in the unit of%).

2.6. PV material flows

We first calculate the dynamic stock and flows of PV modules using the following equations:

$$P_{in}[t] = P[t] - P[t-1] + P_{out}[t] \quad (8)$$

$$P_{out}[t] = \int_{-\infty}^{\infty} P_{in}(t-t') * f(t')dt' \quad (9)$$

Eq. (8) describes the foundational equilibrium between stocks and flows of PV modules. In this equation, P denotes the PV module deployment (in the unit of GWp), which is the in-use stock and the key driver in the material flow analysis model, P_{in} is the annual inflow (annual PV module demand in the unit of GWp), and P_{out} is the annual outflow (annual end-of-life PV modules in the unit of GWp). In the initial year of PV deployment, denoted as year 1, we assume $P[1] = P_{in}[1]$, signifying that the annual demand for PV modules is equal to the PV module deployment/stock. The P_{out} in year t, representing the annual end-of-life PV modules that were deployed in various years before year t, is determined by the cohort and the PV module's lifetime distribution function (refer to Eq. (9)). Here, $t'(t' < t)$ represents the year in which the

PV module was deployed, and $f(t')$ (refer to Eq. (1)) denotes the probability that the PV module deployed in year t' will reach the end of its life in year t.

We then calculate the material flows of PV modules using the following equations:

$$M_{in,j}[t] = \frac{P_{in}[t] * 10^6}{MI_j[t]} \tag{10}$$

$$M_{out,j}[t] = \int_{-\infty}^{\infty} \frac{P_{in}(t-t') * f(t') * 10^6}{MI_j[t]} dt' \tag{11}$$

$$M_{in,\ j,cum} = \sum_{t=2022}^{2050} M_{in,j}[t] \tag{12}$$

$$M_{out,j,\ cum} = \sum_{t=2022}^{2050} M_{out,j}[t] \tag{13}$$

where $M_{in,j}$ is inflow for material type j (annual material demand in the unit of kg), $M_{out,j}$ is the outflow for material type j (annual end of life PV module materials in the unit of kg), $M_{in,\ j,cum}$ is the cumulative inflow for material type j during 2022–2050 (cumulative material demand in the unit of kg), and $M_{out,j,\ cum}$ is cumulative outflow for material type j during 2022–2050 (cumulative end of life PV module materials in the unit of kg).

Finally, we calculate closed-loop recycling potential (CRP) during 2022–2050, which is defined as the ratio of cumulative recovered materials to cumulative material demand, using the following Eq. (14):

$$CRP_j = \frac{M_{out,j,\ cum} * Collection\ rate * Recovery\ rate_j}{M_{in,\ j,cum}} \tag{14}$$

where CRP_j is the closed-loop recycling potential from 2022 to 2050 for material type j (in the unit of%), Collection rate is the percentage of end of life PV modules collected and ready for recycling (in the unit of%), and *Recovery rate*$_j$ is the percentage of end of life material type j that can be recovered by recycling technology (in the unit of%).

3. Results

3.1. PV module deployment

In Section 2.2, we outline the methods used for projecting the future size of global PV module deployment. Fig. 2 displays the results of the projected global PV module deployment until 2050. As of 2022, global cumulative PV module deployment has reached around 1 terawatt peak (TWp) (IRENA, 2023b). This deployment is estimated to generate approximately 1.3 petawatt hours (PWh) of electricity under average irradiation conditions, constituting only 4.5 % (EMBER, 2023) of the worldwide electricity generation in 2022 (29 PWh) (RTOInsider, 2023). In the conservative PV scenario future cumulative deployment holds the potential to achieve 15.5 TWp (IEA, 2021) by 2050 (annual PV module deployment of 0.7 TWp), which is based on the International Energy Agency (IEA) to represent the low bound of PV deployment. In contrast, the optimistic PV scenario, representing the high bound of PV deployment based on Bogdanov et al. (2021), envisions cumulative PV deployment up to 63.4 TW_p by 2050 (annual PV module deployment of 5 TWp). Cumulative PV module deployment diverge by a factor of 4 between the conservative and the optimistic scenarios by 2050. This disparity arises from variations in modeling global electricity generation and the assigned role of PV. In the conservative scenario, PV is estimated to contribute 35 % to the projected 70 PWh global electricity generation, while the optimistic scenario envisions PV's contribution of 69 % to the projected 150 PWh global electricity generation by 2050.

3.2. PV module efficiency

Overall, the PV technology market share-based average module efficiency is projected to increase from 22.6 % in 2022 to 28.7 % in 2050. This result is based on the market shares of various silicon-based PV technologies (please refer to the methods section for details and Supplementary Fig. 1 for results) and the module efficiency projection for each technology (Fig. 3). Note that the efficiency numbers presented in Fig. 3 refer to the market average module efficiency for each technology available in the market, which are often lower than the maximum efficiencies obtained with increased efforts for world record efficiency attempts. As of 2022, Al-BSF typically exhibits a module efficiency of around 18.5 % (Frischknecht et al., 2015). Al-BSF is projected to phase out by 2026 (Fazal and Rubaiee, 2023; Kashyap et al., 2020; VDMA, 2022). On top of Al-BSF, PERC) (Sadhukhan et al., 2021) and TOPCon

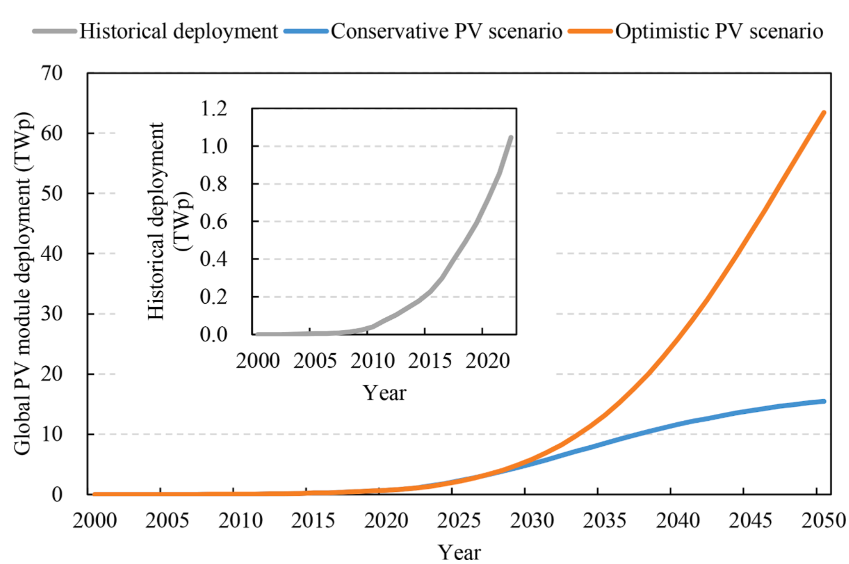

Fig. 2. Global PV module deployment until 2050. The conservative PV scenario is derived from the (IEA, 2021), and the optimistic PV scenario is obtained from (Bogdanov et al., 2021).

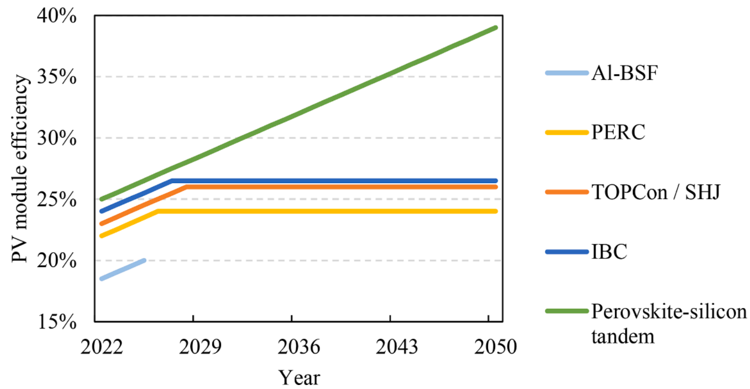

Fig. 3. PV module efficiency projections for various silicon-based PV technologies until 2050. Note PV module efficiency in the figure refers to monofacial modules. The Al-BSF is anticipated to phase out of the market since 2026. TOPCon and SHJ are projected to exhibit identical module efficiency trajectories through 2050. The perovskite-silicon tandem utilizes SHJ as the bottom module and can adopt either a monolithically integrated two-terminal (2T) or a mechanically stacked four-terminal (4T) configuration. Abbreviations include Al-BSF for aluminum back surface field, PERC for passivated emitter and rear contact, TOPCon for tunnel oxide passivated contact, SHJ for silicon heterojunction, and IBC for interdigitated back contact.

(Xu et al., 2022) deploy additional aluminum oxide and silicon-contained layers (silicon nitride, or silicon oxide, or poly-Si) to enhance surface passivation and increase the efficiency of PV modules (Allen et al., 2019). PERC module efficiency, at 22 % (VDMA, 2022) in 2022, is expected to reach 24 % (Hermle et al., 2020) by 2050. TOPCon module efficiency is projected to increase from 23 % (VDMA, 2022) in 2022 to 26 % (Hermle et al., 2020) in 2050. These efficiency projections are accompanied by a market share of 16 % for TOPCon and only 1 % for PERC by 2050. SHJ modules utilize amorphous silicon and indium tin oxide layers to enhance electron collection efficiency (EPFL, 2023). SHJ module efficiency achieved 23 % in 2022 (VDMA, 2022) and is projected to reach 26 % by 2050 (Hermle et al., 2020). The market share for SHJ modules is projected to rise to 63 % by 2050. These market share projections for TOPCon and SHJ in 2050 are based on assumed continuing trends of the ITRPV's market share projection from 2028 to 2031 (VDMA, 2022), which suggests a declining market share for TOPCon and an increasing market share for SHJ. IBC modules put all grid contacts at the rear side and have optimized module efficiency to 24 % (VDMA, 2022) in 2022. IBC module efficiency is expected to reach 26.5 % by 2050, constituting 10 % of the PV market by 2050. Perovskite-silicon tandem modules, integrating a perovskite on top of a SHJ (Shrivastav et al., 2021; Tockhorn et al., 2022), are projected to reach module efficiency of 39 % (PVmagazine, 2023) by 2050. This is technically reasonable since the projected efficiency is below the fundamental module efficiency limit (42.5 %) (Blom et al., 2023) for perovskite-silicon tandem. Perovskite-silicon tandem modules will constitute a 10 % market share by 2050. As the default scenario, we assume that the tandem market is evenly divided between a monolithically integrated two-terminal (2T) configuration and a mechanically stacked four-terminal (4T) configuration, as explained in the methods section.

Note that we present a promising scenario analysis regarding advancements in PV efficiency, particularly for perovskite-silicon tandem technologies. Further research is needed to substantiate claims about significant efficiency improvements. This may include evaluating the feasibility of mass production, the availability of necessary materials, and the economic and logistical aspects of manufacturing.

3.3. Annul material demand

Fig. 4 presents the annual material demand for indium, silver, tin, silicon, aluminum, and copper until 2050, considering a mixed market share of different silicon-based PV technologies. Material demand results for other PV materials are available in Supplementary Fig. 2. Higher PV module deployments in the optimistic PV deployment scenario (indicated by the orange lines in Fig. 4) result in 7.5 times higher annual material demand than in the conservative PV deployment scenario (indicated by the blue lines in Fig. 4) in 2050. When comparing annual demand to global annual production (indicated by the black lines in Fig. 4) it's observed that indium and silver used in the PV sector may surpass global production levels. Tin and silicon require a significant portion of global production, while aluminum and copper require less than 10 % of production. Further discussion can be found in the subsequent section of discussions.

The scenario with material intensity improvement (denoted by the solid line in Fig. 4) can reduce material demand significantly compared to the scenario without material intensity improvement (denoted by the dashed line in Fig. 4). The reduction percentages are related to material intensity trends (in the unit of kg per Wp), which is affected by both PV module efficiency (which determines rated power, in the unit of Wp per m^2) and material mass per module area (in the unit of kg per m^2). The reduction percentage is expected to reach 13 % for indium, tin, and copper in 2050. For these materials, only PV module efficiency increase (see Fig. 3) is considered for decreasing material intensity, resulting in a material intensity reduction factor of 1.1–1.56 during 2022–2050 depending on PV technology. In contrast, for silicon, aluminum, and silver, the reduction percentage in 2050 will be higher (46 % for silicon, 35 % for aluminum, and 30 % for silver). This is due to the consideration of a notable decrease in material mass per module area for these materials, in addition to PV module efficiency increase; material mass per module area holds greater potential for reducing material intensity compared to relying solely on PV module efficiency (see Supplementary Fig. 3 and Supplementary Note 3). Combining material mass per module area and PV module efficiency yields a material intensity reduction factor of 1.7–2.5 for silicon, 1.5–2.1 for aluminum, and 1.5–2 for silver during 2022–2050, depending on the PV technology.

Therefore, with material intensity improvement, the annual material demand is projected to grow from 0.035 kt in 2022 to 1.3–10 kt in 2050 for indium, from 2.7 kt in 2022 to 9.5–71.8 kt for silver, from 10.7 kt in 2022 to 28.7–216.3 kt in 2050 for tin, from 0.3 Mt in 2022 to 0.5–3.7 Mt in 2050 for silicon, from 0.4 Mt in 2022 to 0.9–6.7 Mt for aluminum, and from 0.08 Mt in 2022 to 0.2–1.7 Mt for copper. The corresponding increasing factor is 38–286 for indium, 4–27 for silver, and 2–20 for the remaining PV materials over the period of 2022–2050 (see Supplementary Fig. 4).

3.4. Cumulative material demand

Fig. 5 illustrates the cumulative demand for indium and silver from 2022 to 2050 under various PV technology choices, considering material

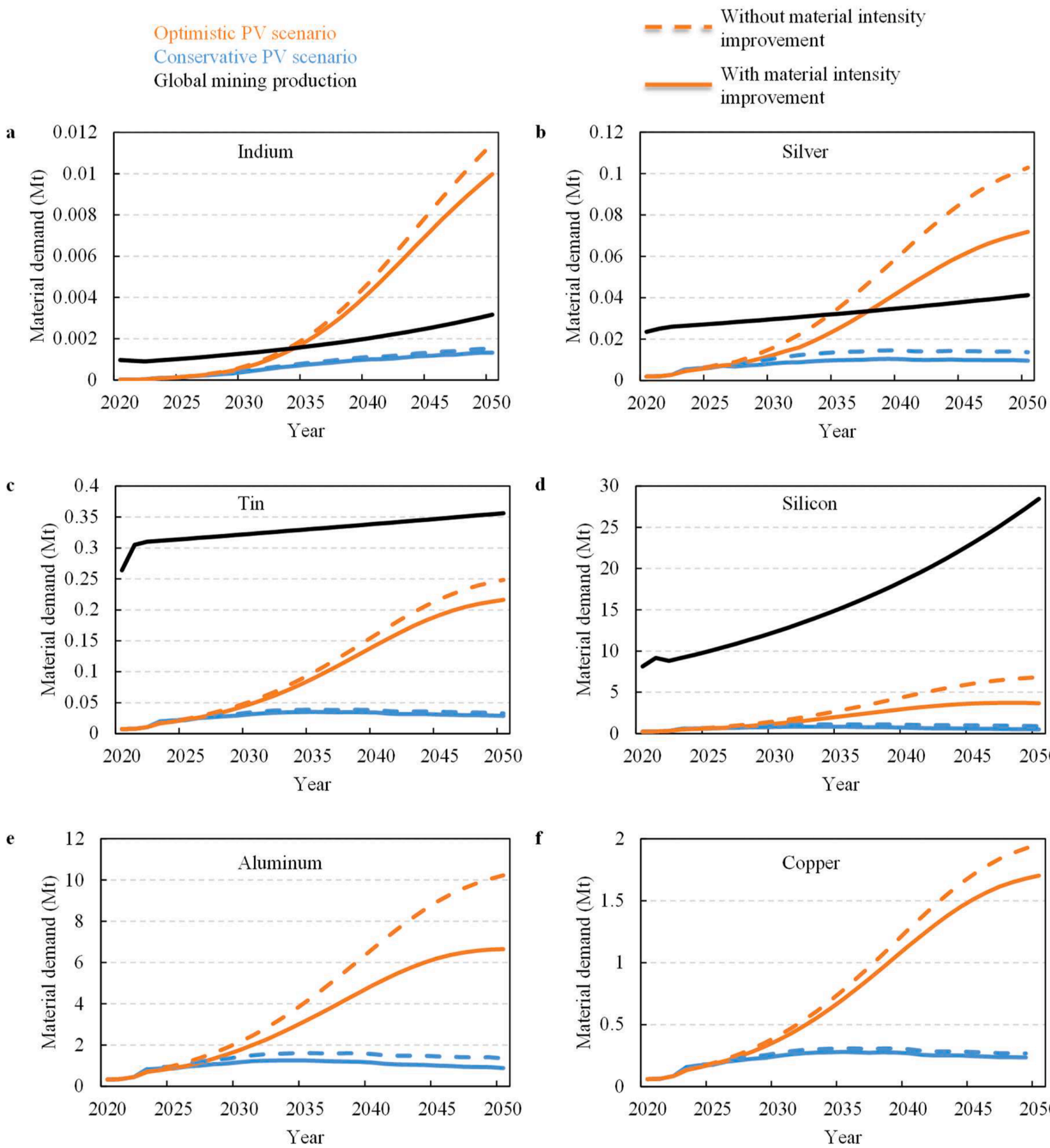

Fig. 4. Annual material demand for global PV modules until 2050, considering scenarios of PV deployment and material intensity. The panels represent annual demand for (**a**) indium, (**b**) silver, (**c**) tin, (**d**) silicon, (**e**) aluminum, and (**f**) copper. Material demand results for other PV materials are available in Supplementary Fig. 2. Historical global mining production data is sourced from USGS (USGS, 2023a, 2023b, 2023c, 2023d, 2023e, 2023f), while the production data beyond 2022 is extrapolated by assuming a continuing annual average growth rate equal to that observed during 2000–2022. We find a substantial surplus in the global mining production of aluminum and copper relative to the demand for them in PV modules; therefore, global mining production data for aluminum and copper exceed the y-axis scale in figures **e** and **f**.

intensity improvement. Supplementary Fig. 5 presents results for other materials. While achieving a 100 % market share for a single PV technology is not practical, the results in Fig. 5 are intended to reveal significant variations in cumulative demand attributed to technology choices. Remarkably, the impact of PV technology choice is more pronounced for indium and silver compared to other materials. In most cases the demand for indium and silver may exceed their available reserves. This issue will be discussed in detail in the subsequent discussions section.

For indium, cumulative demand during 2022–2050 varies from 0 kt for the 100 % PERC/100 % TOPCon cases to 209 kt for the 100 % 4T tandem case (perovskite-silicon tandem in a mechanically stacked four-terminal configuration) in the optimistic PV scenario (Fig. 5a). This variation is attributed to the fact that indium is not required in PERC and TOPCon technologies, while for the 4T tandem, indium is utilized in both the bottom SHJ cell and the top perovskite cell. In the case of perovskite-silicon tandem, choosing a monolithically integrated two-terminal (2T) tandem configuration (i.e., 100 % 2T tandem case), rather than 4T, would lead to lower indium demand. This is because in a 2T configuration, the indium usage in the bottom SHJ can be approximately 40 % less than that of a standard SHJ, while in a 4T configuration, the indium usage in the bottom SHJ remains the same as that of a standard SHJ (please refer to the methods section for further details). The indium demand in the 100 % SHJ case falls between the 100 % 2T tandem case and the 100 % 4T tandem case.

For silver, the cumulative demand during 2022–2050 ranges from 144 kt for the 100 % PERC case in the conservative PV scenario to 1121 kt for the 100 % SHJ case in the optimistic PV scenario (Fig. 5b). TOPCon and SHJ achieve higher module efficiency than PERC, however, this improvement comes at the cost of higher silver usage per module area than PERC. The higher module efficiency in TOPCon and SHJ is not sufficient to offset their higher silver usage, resulting in TOPCon and SHJ exhibiting higher silver material intensity compared to PERC. There is an 84 % and 121 % higher silver demand for the 100 % TOPCon case

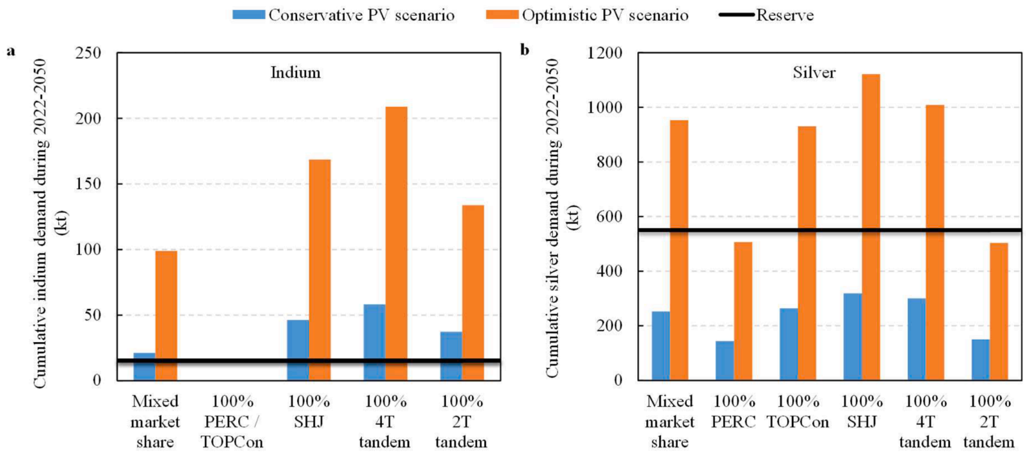

Fig. 5. Cumulative material demand during 2022–2050 for different PV technology choices. Reserve data in 2022 is sourced from USGS (USGS, 2023c, 2023e). The panels represent cumulative demand for (**a**) indium and (**b**) silver. The mixed market share case illustrates the cumulative demand corresponding to the annual demand presented in Fig. 4. Supplementary Fig. 5 reports the cumulative demand results of other PV materials.

and 100 % SHJ case, respectively, compared to the 100 % PERC case. Perovskite-silicon tandem modules in a 4T configuration utilize the same amount of silver per module area as SHJ but achieve higher module efficiency, resulting in lower silver material intensity than SHJ, though still higher than PERC. This leads to a 66–74 % increase in cumulative silver demand during 2022–2050 for the 100 % 4T tandem case compared to the 100 % PERC case. Perovskite-silicon tandem modules in a 2T configuration have the potential to reduce silver usage per module area by 40 % compared to a standard SHJ (Rehman et al., 2023), due to the 2T tandem's approximately half short-circuit current density of SHJ (Rehman et al., 2023) (please refer to the methods section for details). Opting for the 2T configuration, instead of the 4T configuration, can lead to a contrasting conclusion: cumulative silver demand for the 100 % 2T tandem case could be roughly equal to the 100 % PERC case.

3.5. Recycling potentials

Recycling can reduce primary material demand and holds the potential to mitigate material supply risks. To assess the role of recycling, we introduce closed-loop recycling potential (CRP) as the percentage of PV material demand that secondary materials from PV module recycling can fulfill. Our analysis assumes a 100 % collection rate for end-of-life PV modules due to the limitations of real-world data. This assumption allows us to evaluate the potential availability of secondary materials under optimal PV collection conditions. Although the current situation is far from ideal, the collection rate could be significantly improved and approach this ideal condition in the future. Additionally, we explore the impact of recovery rates on CRP. We consider a 'Full Recovery End of Life Photovoltaic' process (Ercole, 2016; LATUNUSSA, C. et al., 2016; Latunussa, C.E.L. et al., 2016), which was demonstrated by R&D pilot lines in the current PV recycling industry. In this recycling process, the recovery rates reach 94 % for silver, 97 % for silicon, 99.4 % for aluminum, 97 % for copper, and 98 % for glass. Additionally, we consider recovery rates of 99.6 % for indium and 98.6 % for tin, which was achieved in lab-scale research (showcasing industrialization potential) (Gu et al., 2017). Note the quality and purity of the recovered materials achieve 99 % purity for silver, metallurgical grade for silicon, and scrap form for aluminum. However, these may not meet the material specifications required for manufacturing new PV modules. Realizing the CRP in industry practice necessitates efforts to advance PV recycling technology and enhance the quality and purity of recovered materials. Our estimates of CRP are generally optimistic and offer an upper bound of future recycling potentials.

Fig. 6 presents the CRP during 2022–2050 for indium, silver, tin, silicon, aluminum, and copper. For CRP of other PV materials, please refer to Supplementary Fig. 6. It is observed from Fig. 6 that the CRP could achieve 6–12 % for indium, 10–22 % for silver, 11–25 % for tin, 14–30 % for silicon, 13–28 % for aluminum, and 11–25 % for copper during 2022–2050, depending on PV deployment scenarios. The CRP in the conservative PV scenario is higher compared to the optimistic PV scenario. This discrepancy arises from the conservative PV scenario approaching a close-to-steady state for new annual PV capacity deployment by 2035, where end-of-life PV module materials can constitute a large fraction of material demand (a fraction of 64 % in 2050). In contrast, the optimistic PV scenario exhibits continuous growth in PV deployment until 2050, where end-of-life materials cover only a small fraction of material demand (a fraction of 20 % in 2050).

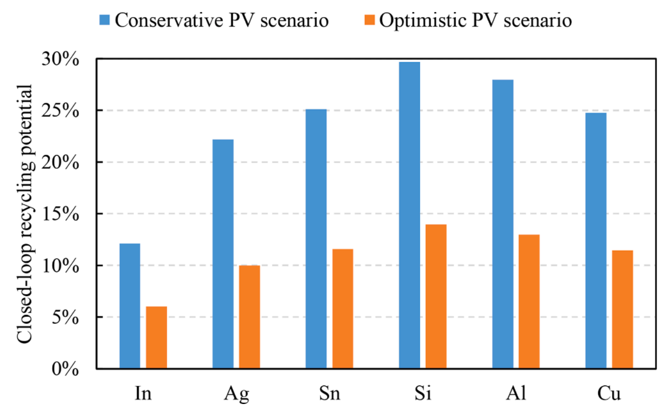

Fig. 6. Closed-loop recycling potential for indium, silver, tin, silicon, aluminum, and copper during 2022–2050. For CRP values of other PV materials, please refer to Supplementary Fig. 6.

4. Discussions

Higher PV deployment in the optimistic PV scenario results in the annual demand for indium and silver potentially exceeding global mining production before 2040 (see Fig. 4). Known reserves in 2022 could be depleted in the optimistic scenario for indium and silver before 2050, and for indium also in the conservative PV scenario with lower PV deployment. Potential supply risks arise for indium and silver, necessitating the rapid scaling up of indium and silver production with an annual average growth rate of 9 % for indium and 3.7 % for silver continuing over the next three decades, despite historical annual average growth rates of 4.6 % (USGS, 2023c) for indium and 1.7 % (USGS, 2023e) for silver. Indium, which is the by-product of mining or refining primary mineral commodities such as copper and zinc, is typically not economical to produce independently (Lokanc et al., 2015). Lengthy lead times in mining operations can impede the supply expansion of indium and silver (Rademeyer et al., 2020). The concentration of indium and silver production, where the top three producing countries account for over 80 % of indium production (China, Korea, and Canada) and over 50 % of silver production (Mexico, China, and Peru), has exposed the supply chain to risks related to geopolitical tensions, trade restrictions, and market fluctuations (IEA, 2022a). Supply risk concerns could also extend to tin and silicon, as these elements require a significant share of global mining production, reaching 70 % for tin and 42 % for silicon in 2050 in the optimistic PV scenario. Silicon, in particular, may face challenges in rapidly expanding the refinement and purification process to yield solar-grade silicon. For aluminum, copper, and other PV materials, their annual production and known reserves exceed the demand from PV modules until 2050. Annual demand for aluminum and copper in the optimistic scenario only requires 10 % and 7 % of global mining production in 2050.

Our estimation of annual indium demand for PV modules in 2050 (1.3–10 kt) is higher than the projections by IEA (2023) (0.11 kt) and Simon et al. (Davidsson and Höök, 2017) (1–4.3 kt) for the same year. Our estimated annual silver demand in 2050 (9.5–71.8 kt) surpasses the estimations by IEA (IEA, 2023) (1.19 kt) and Simon et al. (Davidsson and Höök, 2017) (1–11 kt). Our higher estimates can be primarily attributed to the larger size of PV deployment in our model (15.5 TWp to 63.4 TWp in 2050), in contrast to the IEA's consideration of 15.5 TWp (IEA, 2023) and Simon's adoption of only 9.3 TWp (Davidsson and Höök, 2017) in 2050. Brett et al. (Hallam et al., 2023) use similar PV deployment projections (15–60 TWp by 2050) as ours, and their estimates of cumulative silver demand during 2022–2050 (450–520 kt) fall within our estimation range (252–953 kt). The variation between Brett et al. (Hallam et al., 2023) estimates and ours is probably due to different assumptions on silver material intensity. Comparing material intensity assumptions across studies is challenging due to the limited disclosure of the material compositions for different PV technologies. In our study, the PV material compositions vary annually until 2050 for various PV technologies, including perovskite-silicon tandem (refer to Fig. 1). This novelty underscores the unique contribution of our study in providing dynamic PV material composition data. This data is documented in the Supplementary Data to facilitate open scientific discussion.

Material intensity improvement has proven to be an effective approach for reducing PV material demand, as demonstrated by Fig. 4. However, achieving a cumulative material demand below available reserve solely through this approach is challenging for indium and silver (see Fig. 4) unless there is a further breakthrough in material intensity improvement. Material substitution is another approach to reduce material demand by replacing critical materials with more abundant and sustainable materials (Bontempi, 2017) (ideally without compromising PV efficiency). Combining material intensity improvement and material substitution may provide a more effective and technically feasible option. Fig. 7 shows the boundary conditions of material intensity improvement and material substitution, for reaching a balance between cumulative material demand during 2022–2050 and the available reserves in 2022 for indium (Fig. 7a) and silver (Fig. 7b), without considering recycling impact. For indium, material intensity improvement as high as 40 % (improve to 1.9 mg/W by 2050), or material substitution as high as 29 %, can achieve a balance of demand and reserve in the conservative PV scenario. These numbers increase to 550 % for material intensity improvement (improve to 0.39 mg/W by 2050, which is technically feasible as it is equivalent to about 9 nm thickness of ITO per face according to (Zhang et al., 2021)) and 85 % for material substitution in the optimistic PV scenario. A technically feasible option for achieving indium's balance of demand and reserve in the optimistic PV scenario could involve reducing the thickness of indium-contained layer in PV modules by 67 % (Han et al., 2022a) (material intensity improvement as high as 50 % to reach 1.7 mg/W by 2050), and simultaneously substituting approximately 75 % of the indium-contained layer with non-indium-contained layer like aluminum zinc oxide (Murdoch et al., 2009). For silver, balance of demand and reserve can be reached through either a 42 % material substitution or a 73 % material intensity improvement (improved from 14.7 mg/W to 8.5 mg/W in 2050) in the optimistic PV scenario. Substituting silver printing with copper plating or printing could offer a technically viable solution (Lennon et al., 2013). PV modules incorporating substitution options for silver and indium generally have slightly lower efficiencies and higher degradation rates, which may lead to higher material demand than our modeling results suggest. However, many R&D efforts (Han et al., 2022b; Horzel et al., 2015; Li et al., 2021; Peibst et al., 2023; Zhang et al., 2021) aim to address these issues and remove barriers to scaling up PV deployment.

This study acknowledges several limitations that necessitate further research. The wide range of PV deployment sizes shown by the conservative and optimistic PV scenarios leads to large uncertainty in PV material demand projections. This uncertainty can be reduced by using consistent energy system model and policy assumptions (Jaxa-Rozen and Trutnevyte, 2021) to establish a consensus or at least a narrower range for future PV deployment size. One limitation is that we do not consider potential changes in material composition due to PV efficiency improvements and other factors. Higher efficiency modules often require advanced materials and techniques, altering the types and quantities of materials used. As efficiency increases, material composition may be adjusted to optimize performance, cost, and durability. Another limitation is the assumption of a constant thickness for indium-contained layers due to limited available data. Incorporating a dynamically decreasing thickness of indium-contained layers in our model would project a lower indium demand. Additionally, this research

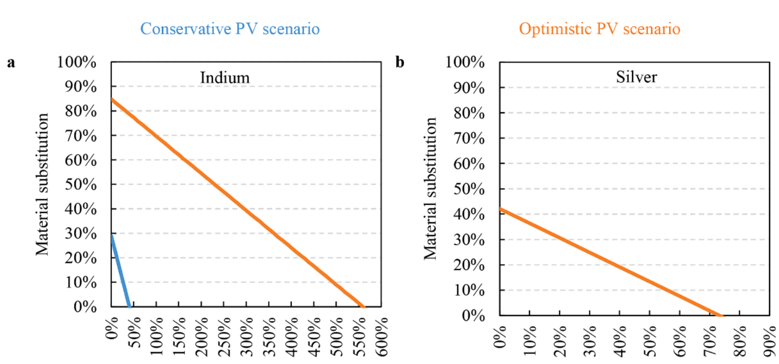

Fig. 7. Boundary conditions for material intensity improvement and material substitution to reach a balance between cumulative material demand during 2022–2050 and the available reserve in 2022. (**a**) indium and (**b**) silver.

focuses exclusively on silicon-based PV module technology, neglecting the potential impact of other PV technologies (e.g., GaAs, InP, CIGS, CdTe, etc. (Polman et al., 2016)) that may require rare earth elements. While demand for aluminum and copper from the PV modules seems manageable compared to the current supply, future research should also investigate aluminum and copper demand from power electronics in PV converters and inverters (Lennon et al., 2022), mounting structures (Lennon et al., 2022), and transmission cables (Chen et al., 2023).

CRediT authorship contribution statement

Chengjian Xu: Writing – review & editing, Writing – original draft, Visualization, Validation, Resources, Methodology, Investigation, Formal analysis, Data curation, Conceptualization. **Olindo Isabella:** Writing – review & editing, Supervision, Methodology, Data curation. **Malte Ruben Vogt:** Writing – review & editing, Validation, Supervision, Methodology, Data curation, Conceptualization.

Declaration of competing interest

The authors declare the following financial interests/personal relationships which may be considered as potential competing interests: Chengjian Xu reports financial support was provided by Delft University of Technology. If there are other authors, they declare that they have no known competing financial interests or personal relationships that could have appeared to influence the work reported in this paper.

Data availability

All data supporting the findings of the present study are available within the paper and its supplementary material.

Acknowledgements

TU Delft's Climate Action Program Flagship project "Materials for circular renewable energy technologies" supported this work. Chengjian Xu also acknowledges Yifeng Zhao and Liqi Cao for their assistance in understanding the basic structures and components of PV technology at the beginning of this work.

Supplementary materials

Supplementary material associated with this article can be found, in the online version, at doi:10.1016/j.resconrec.2024.107824.

References

Allen, T.G., Bullock, J., Yang, X., Javey, A., De Wolf, S., 2019. Passivating contacts for crystalline silicon solar cells. Nat. Energy 4 (11), 914–928.
Ballif, C., Haug, F.-J., Boccard, M., Verlinden, P.J., Hahn, G., 2022. Status and perspectives of crystalline silicon photovoltaics in research and industry. Nat. Rev. Mater. 7 (8), 597–616.
Basore, P., Feldman, D., 2022. Solar photovoltaics: supply chain deep dive assessment. United States.
Blom, Y., Vogt, M.R., Ruiz Tobon, C.M., Santbergen, R., Zeman, M., Isabella, O., 2023. Energy loss analysis of two-terminal tandem PV systems under realistic operating conditions—revealing the importance of fill factor gains. Sol. RRL. 7 (8), 2200579.
BloombergNEF, 2022. Solar –10 Predictions for 2022. https://about.bnef.com/blog/solar-10-predictions-for-2022/.
Bogdanov, D., Ram, M., Aghahosseini, A., Gulagi, A., Oyewo, A.S., Child, M., Caldera, U., Sadovskaia, K., Farfan, J., De Souza Noel Simas Barbosa, L., Fasihi, M., Khalili, S., Traber, T., Breyer, C., 2021. Low-cost renewable electricity as the key driver of the global energy transition towards sustainability. Energy 227, 120467.
Bontempi, E., 2017. Raw Materials Substitution Sustainability. Springer.
Chen, Z., Kleijn, R., Lin, H.X., 2023. Metal requirements for building electrical grid systems of global wind power and utility-scale solar photovoltaic until 2050. Environ. Sci. Technol. 57 (2), 1080–1091.
Choi, C.H., Cao, J., Zhao, F., 2016. System dynamics modeling of indium material flows under wide deployment of clean energy technologies. Resour. Conserv. Recycl. 114, 59–71.
Davidsson, S., Höök, M., 2017. Material requirements and availability for multi-terawatt deployment of photovoltaics. Energy Policy 108, 574–582.
DNV, 2019. Utility-scale solar PV: from big to biggest. https://brandcentral.dnv.com/dl/gallery/10651/others/b52a39d504d14802afbb43f522f44149/b52a39d504d14802afbb43f522f44149_low.pdf?f=DNV_GL_Feature_Utility_Solar_Feb_19_web.pdf.
Duan, H., Wang, J., Liu, L., Huang, Q., Li, J., 2016. Rethinking China's strategic mineral policy on indium: implication for the flat screens and photovoltaic industries. Progr. Photovolt. Res. Appl. 24 (1), 83–93.
Dubey, S., Jadhav, N.Y., Zakirova, B., 2013. Socio-economic and environmental impacts of silicon based photovoltaic (PV) technologies. Energy Procedia 33, 322–334.
Dullweber, T., Stöhr, M., Kruse, C., Haase, F., Rudolph, M., Beier, B., Jäger, P., Mertens, V., Peibst, R., Brendel, R., 2020. Evolutionary PERC+ solar cell efficiency projection towards 24% evaluating shadow-mask-deposited poly-Si fingers below the Ag front contact as next improvement step. Solar Energy Mater. Solar Cells 212, 110586.
Elshkaki, A., Shen, L., 2019. Energy-material nexus: the impacts of national and international energy scenarios on critical metals use in China up to 2050 and their global implications. Energy 180, 903–917.
EMBER, 2023. Global electricity review 2023. https://ember-climate.org/insights/research/global-electricity-review-2023/#supporting-material.
EPFL, 2023. Silicon-based heterojunction solar cells. https://www.epfl.ch/labs/pvlab/research/heterojunction_solar_cells/. 2023).
Ercole, P., 2016. FRELP 2 Project - full recovery end of life photovoltaic.
European, C., Market, Directorate-General for Internal, Smes, I.E., Grohol, M., Veeh, C., 2023. Study On the Critical Raw Materials For the EU 2023 – Final report. Publications Office of the European Union.
European, C., Joint Research, C., Alves Dias, P., Pavel, C., Plazzotta, B., Carrara, S., 2020. Raw Materials Demand For Wind and Solar PV Technologies in the Transition Towards a Decarbonised Energy System. Publications Office.
European, C., Joint Research, C., Blagoeva, D., Marmier, A., Alves Dias, P., Pavel, C., 2016. Assessment of Potential Bottlenecks Along the Materials Supply Chain For the Future Deployment of Low-Carbon Energy and Transport Technologies in the EU – Wind power, Photovoltaic and Electric Vehicles technologies, Time Frame 2015 - 2030. Publications Office.
European, C., Joint Research, C., Chatzipanagi, A., Jaeger-Waldau, A., Cleret de Langavant, C., Letout, S., Latunussa, C., Mountraki, A., Georgakaki, A., Ince, E., Kuokannen, A., Shtjefni, D., 2022. Clean Energy Technology Observatory, Photovoltaics in the European Union – Status report On Technology development, trends, Value Chains and Markets –2022. Publications Office of the European Union.
Fazal, M.A., Rubaiee, S., 2023. Progress of PV cell technology: feasibility of building materials, cost, performance, and stability. Solar Energy 258, 203–219.
Frischknecht, R., Itten, R., Sinha, P., de Wild-Scholten, M., Zhang, J., Heath, G.A., Olson, C., 2015. Life Cycle Inventories and Life Cycle Assessments of Photovoltaic Systems. International Energy Agency (IEA), United States, Paris, France.
Goe, M., Gaustad, G., 2014. Identifying critical materials for photovoltaics in the US: a multi-metric approach. Appl. Energy 123, 387–396.
Gómez, M., Xu, G., Li, J., Zeng, X., 2023. Securing indium utilization for high-tech and renewable energy industries. Environ. Sci. Technol. 57 (6), 2611–2624.
GOV.UK, 2023. Resilience for the future: the UK's critical minerals strategy. https://www.gov.uk/government/publications/uk-critical-mineral-strategy/resilience-for-the-future-the-uks-critical-minerals-strategy#fn:9.
Gu, S., Fu, B., Dodbiba, G., Fujita, T., Fang, B., 2017. A sustainable approach to separate and recover indium and tin from spent indium–tin oxide targets. RSC Adv. 7 (82), 52017–52023.
Guzik, K., Burkowicz, A., Szlugaj, J., 2022. The EU's demand for selected critical raw materials used in the photovoltaic industry. Gospodarka Surowcami Mineralnymi - Min. Resour. Manage. 38 (2), 31–59.
Hallam, B., Kim, M., Zhang, Y., Wang, L., Lennon, A., Verlinden, P., Altermatt, P.P., Dias, P.R., 2023. The silver learning curve for photovoltaics and projected silver demand for net-zero emissions by 2050. Progr. Photovolt. Res. Appl. 31 (6), 598–606.
Han, C., Santbergen, R., van Duffelen, M., Procel, P., Zhao, Y., Yang, G., Zhang, X., Zeman, M., Mazzarella, L., Isabella, O., 2022a. Towards bifacial silicon heterojunction solar cells with reduced TCO use. Progr. Photovolt. Res. Appl. 30 (7), 750–762.
Han, C., Yang, G., Procel, P., O'Connor, D., Zhao, Y., Gopalakrishnan, A., Zhang, X., Zeman, M., Mazzarella, L., Isabella, O., 2022b. Controllable simultaneous bifacial Cu-plating for high-efficiency crystalline silicon solar cells. Sol. RRL. 6 (6), 2100810.
Heidari, S.M., Anctil, A., 2021. Material requirement and resource availability for silicon photovoltaic laminate manufacturing in the next 10 years. In: 2021 IEEE 48th Photovoltaic Specialists Conference (PVSC), pp. 1768–1772.
Hermle, M., Feldmann, F., Bivour, M., Goldschmidt, J.C., Glunz, S.W., 2020. Passivating contacts and tandem concepts: approaches for the highest silicon-based solar cell efficiencies. Appl. Phys. Rev. 7 (2), 021305.
Hernandez, R.R., Easter, S.B., Murphy-Mariscal, M.L., Maestre, F.T., Tavassoli, M., Allen, E.B., Barrows, C.W., Belnap, J., Ochoa-Hueso, R., Ravi, S., Allen, M.F., 2014. Environmental impacts of utility-scale solar energy. Renew. Sustain. Energy Rev. 29, 766–779.
Horzel, J., Bay, N., Passig, M., Kühnlein, H., Yuan, S., Verlinden, P., 2015. Industrial Si solar cells with Cu based plated contacts. In: 2015 IEEE 42nd Photovoltaic Specialist Conference (PVSC), pp. 1–3.
IEA, 2021. Net zero by 2050 data explorer. https://www.iea.org/data-and-statistics/data-tools/net-zero-by-2050-data-explorer.
IEA, 2022a. Solar PV global supply chains. https://www.iea.org/reports/solar-pv-global-supply-chains.

IEA, 2022b. Solar PV power capacity in the Net Zero Scenario, 2010-2030. https://www.iea.org/data-and-statistics/charts/solar-pv-power-capacity-in-the-net-zero-scenario-2010-2030.

IEA, 2023. Critical minerals data explorer. https://www.iea.org/data-and-statistics/data-tools/critical-minerals-data-explorer.

IRENA, 2023a. Geopolitics of the energy transition: critical materials. https://mc-cd8320d4-36a1-40ac-83cc-3389-cdn-endpoint.azureedge.net/-/media/Files/IRENA/Agency/Publication/2023/Jul/IRENA_Geopolitics_energy_transition_critical_materials_2023.pdf?rev=f289d177cda14b9aaf2d1b4c074798b4.

IRENA, 2023b. Renewable energy technologies data. https://www.irena.org/Data/View-data-by-topic/Capacity-and-Generation/Technologies.

Jaxa-Rozen, M., Trutnevyte, E., 2021. Sources of uncertainty in long-term global scenarios of solar photovoltaic technology. Nat. Clim. Chang. 11 (3), 266–273.

Kashyap, S., Madan, J., Pandey, R., Sharma, R., 2020. Comprehensive study on the recent development of PERC solar cell. In: 2020 47th IEEE Photovoltaic Specialists Conference (PVSC), pp. 2542–2546.

Kügerl, M.-T., Hitch, M., Gugerell, K., 2023. Responsible sourcing for energy transitions: discussing academic narratives of responsible sourcing through the lens of natural resources justice. J. Environ. Manage. 326, 116711.

LATUNUSSA, C., MANCINI, L., BLENGINI, G., ARDENTE, F., PENNINGTON, D., 2016. Analysis of material recovery from silicon photovoltaic panels.

Latunussa, C.E.L., Ardente, F., Blengini, G.A., Mancini, L., 2016. Life Cycle Assessment of an innovative recycling process for crystalline silicon photovoltaic panels. Solar Energy Mater. Solar Cells 156, 101–111.

Lennon, A., Lunardi, M., Hallam, B., Dias, P.R., 2022. The aluminium demand risk of terawatt photovoltaics for net zero emissions by 2050. Nat. Sustain. 5 (4), 357–363.

Lennon, A., Yao, Y., Wenham, S., 2013. Evolution of metal plating for silicon solar cell metallisation. Progr. Photovolt. Res. Appl. 21 (7), 1454–1468.

Li, S., Pomaska, M., Lambertz, A., Duan, W., Bittkau, K., Qiu, D., Yao, Z., Luysberg, M., Steuter, P., Köhler, M., Qiu, K., Hong, R., Shen, H., Finger, F., Kirchartz, T., Rau, U., Ding, K., 2021. Transparent-conductive-oxide-free front contacts for high-efficiency silicon heterojunction solar cells. Joule 5 (6), 1535–1547.

Li, W., Adachi, T., 2019. Evaluation of long-term silver supply shortage for c-Si PV under different technological scenarios. Nat. Resour. Model 32 (1), e12176.

Lo Piano, S., Saltelli, A., van der Sluijs, J.P., 2019. Silver as a constraint for a large-scale development of solar photovoltaics? Scenario-making to the year 2050 supported by expert engagement and global sensitivity analysis. Front. Energy Res. 7.

Lokanc, M., Eggert, R., Redlinger, M., 2015. The availability of indium: the present, medium term, and long term. United States.

Lowe, R.J., Drummond, P., 2022. Solar, wind and logistic substitution in global energy supply to 2050 – barriers and implications. Renew. Sustain. Energy Rev. 153, 111720.

Murdoch, G.B., Hinds, S., Sargent, E.H., Tsang, S.W., Mordoukhovski, L., Lu, Z.H., 2009. Aluminum doped zinc oxide for organic photovoltaics. Appl. Phys. Lett. 94 (21), 213301.

Nassar, N.T., Wilburn, D.R., Goonan, T.G., 2016. Byproduct metal requirements for U.S. wind and solar photovoltaic electricity generation up to the year 2040 under various Clean Power Plan scenarios. Appl. Energy 183, 1209–1226.

Peibst, R., Haase, F., Min, B., Hollemann, C., Brendemühl, T., Bothe, K., Brendel, R., 2023. On the chances and challenges of combining electron-collecting nPOLO and hole-collecting Al-p+ contacts in highly efficient p-type c-Si solar cells. Progr. Photovolt. Res. Appl. 31 (4), 327–340.

Polman, A., Knight, M., Garnett, E.C., Ehrler, B., Sinke, W.C., 2016. Photovoltaic materials: present efficiencies and future challenges. Science (1979) 352 (6283), aad4424.

PVmagazine, 2023. Perovskite-silicon tandem solar cells have practical efficiency potential of 39.5%. https://www.pv-magazine.com/2023/11/30/perovskite-silicon-tandem-solar-cells-have-practical-efficiency-potential-of-39-5/.

Rademeyer, M.C., Minnitt, R.C.A., Falcon, R.M.S., 2020. A characterisation of the mechanisms transforming capital investment into productive capacity in mining projects with long lead-times. Min. Econ. 33 (3), 349–357.

Ramírez-Márquez, C., Villicaña-García, E., Cansino-Loeza, B., Segovia-Hernández, J.G., Ponce-Ortega, J.M., 2020. Inherent occupational health hazards in the production of solar grade silicon. Process Safety Environ. Prot. 142, 285–294.

Rehman, A.u., Van Kerschaver, E.P., Aydin, E., Raja, W., Allen, T.G., De Wolf, S., 2023. Electrode metallization for scaled perovskite/silicon tandem solar cells: challenges and opportunities. Progr. Photovolt. Res. Appl. 31 (4), 429–442.

Ren, K., Tang, X., Höök, M., 2021. Evaluating metal constraints for photovoltaics: perspectives from China's PV development. Appl. Energy 282, 116148.

Resources, C.M.o.L.a., 2016. The Ministry of Land and Resources has identified 24 strategic minerals. https://www.gov.cn/xinwen/2016-11/30/content_5140509.htm#:~:text=%E5%88%97%E5%85%A5%E6%88%98%E7%95%A5%E6%80%A7%E7%9F%BF%E4%BA%A7%E7%9B%AE,%E6%99%B6%E8%B4%A8%E7%9F%B3%E5%A2%A8%E3%80%81%E8%90%A4%E7%9F%B3%E3%80%82.

RTOInsider, 2023. IEA: renewables to Provide 90% of World's New Power Generation. https://www.rtoinsider.com/31596-iea-renewables-worlds-new-power-generation/.

Sadhukhan, S., Acharyya, S., Panda, T., Mandal, N.C., Bose, S., Nandi, A., Das, G., Maity, S., Chaudhuri, P., Chakraborty, S., Saha, H., 2021. Evaluation of dominant loss mechanisms of PERC cells for optimization of rear passivating stacks. Surf. Interfaces. 27, 101496.

Shrivastav, N., Madan, J., Pandey, R., Shalan, A.E., 2021. Investigations aimed at producing 33% efficient perovskite–silicon tandem solar cells through device simulations. RSC Adv. 11 (59), 37366–37374.

Smith, B., Margolis, R.M., 2019. Expanding the photovoltaic supply chain in the United States: opportunities and challenges. United States.

Tan, V., Dias, P.R., Chang, N., Deng, R., 2022. Estimating the lifetime of solar photovoltaic modules in Australia, Sustainability.

Tockhorn, P., Sutter, J., Cruz, A., Wagner, P., Jäger, K., Yoo, D., Lang, F., Grischek, M., Li, B., Li, J., Shargaieva, O., Unger, E., Al-Ashouri, A., Köhnen, E., Stolterfoht, M., Neher, D., Schlatmann, R., Rech, B., Stannowski, B., Albrecht, S., Becker, C., 2022. Nano-optical designs for high-efficiency monolithic perovskite–silicon tandem solar cells. Nat. Nanotechnol. 17 (11), 1214–1221.

USDOE, 2023. What Are Critical Materials and Critical Minerals? USDOE.

USGS, 2023a. Aluminum statistics and information. https://www.usgs.gov/centers/national-minerals-information-center/aluminum-statistics-and-information.

USGS, 2023b. Copper statistics and information. https://www.usgs.gov/centers/national-minerals-information-center/copper-statistics-and-information.

USGS, 2023c. Indium statistics and information. https://www.usgs.gov/centers/national-minerals-information-center/indium-statistics-and-information.

USGS, 2023d Silicon statistics and information. https://www.usgs.gov/centers/national-minerals-information-center/silicon-statistics-and-information.

USGS, 2023e. Silver Statistics and Information. https://www.usgs.gov/centers/national-minerals-information-center/silver-statistics-and-information.

USGS, 2023f. Tin statistics and information. https://www.usgs.gov/centers/national-minerals-information-center/tin-statistics-and-information.

VDMA, 2022. International Technology Roadmap for Photovoltaic (ITRPV). https://www.vdma.org/international-technology-roadmap-photovoltaic.

WaferWorld, 2020. How do thin silicon wafers help make solar cells more accessible for everyone? WaferWorld.

Weckend, S., Wade, A., Heath, G.A., 2016. End of Life Management: Solar Photovoltaic Panels. International Energy Agency (IEA), United States, Paris, France.

Xu, J., Chen, C., Liu, C., Chen, J., Liu, Z., Yuan, X., Li, H., 2022. High efficiency TOPCon solar cells with micron/nano-structured emitter for a balance of light-trapping and surface passivation. Solar Energy Mater. Solar Cells 238, 111606.

Yuan, X., Su, C.-W., Umar, M., Shao, X., LobonŢ, O.-R., 2022. The race to zero emissions: can renewable energy be the path to carbon neutrality? J. Environ. Manage. 308, 114648.

Zhang, Y., Kim, M., Wang, L., Verlinden, P., Hallam, B., 2021. Design considerations for multi-terawatt scale manufacturing of existing and future photovoltaic technologies: challenges and opportunities related to silver, indium and bismuth consumption. Energy Environ. Sci. 14 (11), 5587–5610.

Zhou, J., Huang, Q., Ding, Y., Hou, G., Zhao, Y., 2022. Passivating contacts for high-efficiency silicon-based solar cells: from single-junction to tandem architecture. Nano Energy 92, 106712.